Collisional Effects on Electron Trajectories in Crossed-Field Devices

Allison M. Komrska[1], Lorin I. Breen[2,3], Amanda M. Loveless[1], Keith L. Cartwright[4], and Allen L. Garner[1,3,5]

[1]*School of Nuclear Engineering, Purdue University, West Lafayette, Indiana 47906, USA*

[2]*School of Health Sciences, Purdue University, West Lafayette, Indiana 47907, USA*

[3]*Department of Agricultural and Biological Engineering, Purdue University, West Lafayette, Indiana 47907, USA*

[4]*Sandia National Laboratories, Albuquerque, New Mexico 87123, USA*

[5]*Elmore Family School of Electrical and Computer Engineering, West Lafayette, Indiana 47907 USA*

Correspondence and requests for materials should be addressed to A. L. G (email: algarner@purdue.edu)

Crossed-field diodes (CFDs) are used in multiple high-power applications and are characterized by an applied magnetic field orthogonal to the electric field, induced by the applied voltage across the anode-cathode gap. In vacuum, the Hull cutoff magnetic field (HCMF) represents the maximum applied magnetic field for which an electron from the cathode can reach the anode. This study investigates the effects of non-vacuum conditions on electron trajectories by introducing electron mobility, which represents particle collisions. We used numerical solutions of the electron force law and particle-in-cell simulations (XPDP1) to assess electron motion for various electron mobilities. For magnetic fields above the HCMF in vacuum, reducing the electron mobility increases the time for an electron emitted from the cathode to reach the anode. Reducing mobility below 22 C s/kg eliminates the HCMF for any magnetic field, meaning that an emitted electron will always cross the gap. We derived the magnetic field, mobility, and electron transit time corresponding to this condition by solving for the condition when the electron velocity in the direction across the anode-cathode gap going to zero at the anode. A parametric study of these conditions using theory and XPDP1 is performed under different gap distances, voltages, and magnetic fields.

Crossed-field devices, where a magnetic field is introduced orthogonal to a device's electric field, have many applications such as crossed-field amplifiers [1], high-power microwave sources [2], and magnetically insulated transmission lines for pulsed-power systems [2]. In a standard diode at

vacuum, an electron emitted from the cathode will travel directly across the gap. Introducing a magnetic field causes the electron to curve as it crosses the gap. The emitted electron will cross the gap until a sufficiently strong magnetic field is applied such that the electron just barely reaches the anode with zero velocity across the gap. This magnetic field is referred to as the Hull cutoff magnetic field B_H[3].

For magnetic field $B > B_H$, an electron emitted from the cathode will not reach the anode and will instead return to the cathode in a cycloidal orbit. Such a diode is referred to as magnetically insulated. Many practical devices, such as the U. S. Navy's Aegis radar system, operate at $B > B_H$[4].

Interestingly, magnetic insulation may be eliminated by system perturbations. For instance, tilting the applied magnetic field introduces a velocity component parallel to the electric field such that an emitted electron always reaches the anode regardless of magnetic field strength [5]. Recent simulation and theory studies also demonstrated that introducing a series resistor altered electron trajectories and the maximum current in the crossed-field gap for $B \approx B_H$ [6]. Introducing ions in the gap also changes electron behavior in a crossed-field gap [7]. Particle-in-cell simulations show that introducing pressure into a crossed-field gap eliminates the Hull cutoff, although the time for the electrons to cross the gap may be quite long (>10^{-6} s) depending on application [2].

Practical vacuum electronics devices do not operate in perfect vacuum, so recent studies have examined the implications of collisions on the maximum current permissible in a diode, defined as the space-charge limited current (SCLC). One studied unified SCLC in vacuum, given by the Child-Langmuir (CL) law, with the SCLC with collisions, given by the Mott-Gurney (MG) law [8] by incorporating collisions into electron motion by introducing electron mobility as a friction term. Subsequent analysis introduced field emission by using the Fowler-Nordheim (FN)

law as the source current density to demonstrate transitions between CL, MG, and FN [9] before introducing a series resistor [10], thermionic emission through the Richardson-Laue-Dushman (RLD) equation [11], and photoemission through the Fowler-DuBridge (FD) equation [12]. This technique, referred to as "nexus theory", has recently been applied to a crossed-field device to demonstrate the transitions between RLD, FN, and limiting current for a crossed-field diode [13]. The limiting current for a crossed-field diode differs from CL and also differs between non-magnetically insulated ($B < B_H$) [14] and magnetically insulated ($B > B_H$) [15][16] conditions. Applying nexus theory to a crossed-field diode required separately accounting for each of these cases.

Because introducing collisions into a crossed-field diode eliminates magnetic insulation, introducing electron mobility into the force law as done for the non-magnetic case will complicate behavior. The closest analog is the tilted magnetic field, where the tilt causes the electrons to loop around as the traverse the diode [5]. Understanding the implications of electron mobility on electron trajectories and magnetic insulation is critical prior to assessing potential implications on limiting current.

In this paper, we start from the electron force law for a crossed-field gap with collisions and solve for the traditional Hull cutoff condition corresponding to the electron reaching the anode with the velocity in the direction along the electric field as zero. We demonstrate that while this traditional Hull cutoff condition still exists for sufficiently large mobility, it does not indicate the onset of magnetic insulation as in vacuum, but instead represents a bifurcation in the transit time from a smooth increase with increasing B for $B < B_H$and a rapid increase with increasing B for $B > B_H$.

Results

Theoretical analysis and results. Consider a one-dimensional planar diode system, which, in Cartesian coordinates, locates the cathode at x = 0 and the anode at $x = D$, as shown in Figure 1. There is an external magnetic field, $\vec{B} = B_z\hat{z}$, applied into the system. The cathode is held at a potential $\phi = 0$ and the anode held at $\phi = V$, resulting in an electric field $\vec{E} = E_x\hat{x} = V/D$ $\hat{x}$ since we assume a sufficiently low injection current to avoid space-charge buildup.

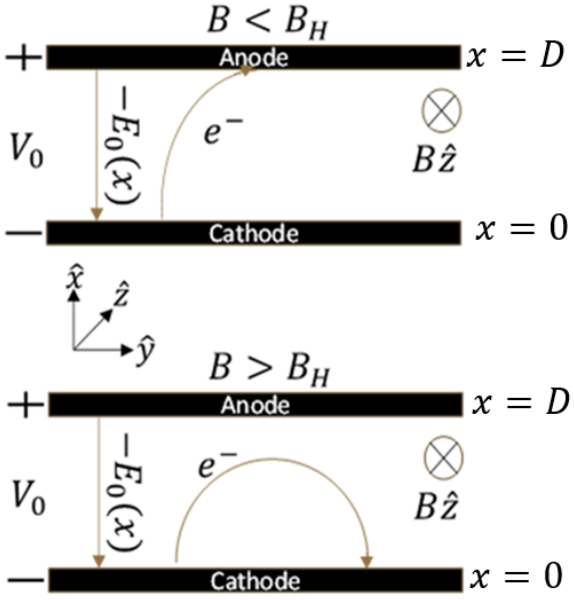

Figure 1. Cathode-anode system showing external magnetic field $\vec{B} = B_z\hat{z}$, gap distance D, voltage V_0, and electric field $E_x\hat{x} = V/D\hat{x}$.

From the Lorentz force law, the force $\vec{F}$ on the electron is given by

$$\vec{F} = q\left(\vec{E} + \vec{v} \times \vec{B}\right). \tag{1}$$

Equating (1) with Newton's Second law yields two differential equations,

$$x'' = \frac{eE_x}{m} - \frac{eB_z}{m}y', y'' = \frac{eB_z}{m}x' \tag{2}$$

where e and m are the electron charge and mass, respectively. Solving the differential equations using initial conditions $x(0) = 0$ and $x'(0) = 0$, where $\Omega = eB/m$ is the cyclotron frequency, yields

$$x(t) = \frac{eE_x}{m\Omega^2}(1 - \cos\Omega t),\ x'(t) = \frac{eE}{m\Omega^2}\sin\Omega t. \tag{3}$$

The Hull cutoff condition is defined by an electron reaching the anode at $x = D$ at time $t = \tau$ with zero velocity in the x-direction, given symbolically as

$$x(\tau) = D,\ v_x = x'(\tau) = 0. \tag{4}$$

Combining (3) and (4) gives

$$B_H = \sqrt{\frac{2mV}{eD^2}}. \tag{5}$$

Because devices cannot always achieve perfect vacuum conditions, we will incorporate electron collisions with neutral particle by introducing the electron mobility μ as a "frictional" component in an electron's trajectory. We can write Poisson's equation as

$$\frac{d^2\phi}{dx^2} = \frac{\rho}{\epsilon_0} \tag{6}$$

and continuity as

$$J = \rho v, \tag{7}$$

where ρ is the electron charge density, and the electron force law becomes

$$mx''(t) = e\left(\frac{d\varphi}{dx}\right) + ey'(t)B_z - \frac{x'(t)}{\mu}, \tag{8}$$

and

$$my''(t) = -ex'(t)B_z - \frac{y'(t)}{\mu}. \tag{9}$$

To eliminate parameters and facilitate analysis, we define

$$\begin{gathered}\varphi = \frac{mD^2\Omega^2}{e}\overline{\varphi};\ \ J = \frac{m\varepsilon_0\Omega^3 D}{e}\overline{J};\ x = D\overline{x}\,;\ y = y_0\overline{y}\,;\ t = \frac{1}{\Omega}\overline{t}\,;\ \mu = \frac{et}{m}\overline{\mu};\\ E = \frac{d\varphi}{dx};\ u_x = \Omega \mathrm{D}\overline{u}_x\,;\ \ y_0 = D;\ \ u_y = \Omega \mathrm{y}_0\overline{u}_y,\end{gathered} \tag{10}$$

where the terms with bars are nondimensional.

Combining equations (1), (6), and (7), and nondimensionalizing with equation (8) through yields

$$\frac{d^2\overline{\phi}}{d\overline{x}^2} = \frac{\overline{J}}{\overline{u}_x}; \frac{d\overline{u}_x}{d\overline{t}} = \frac{d\overline{\phi}}{d\overline{x}} + \overline{u}_y - \frac{\overline{u}_x}{\overline{\mu}}; \frac{d\overline{u}_y}{d\overline{t}} = -\overline{u}_x - \frac{\overline{u}_y}{\overline{\mu}}\,. \tag{11}$$

Hull cutoff initial conditions (5) are applied and the differential equations are solved for nondimensional electron position and velocity:

$$\overline{x}(\overline{t}) = \frac{e^{-\overline{t}/\overline{\mu}}\,\overline{\mu}\,\overline{V}\left(-e^{\overline{t}/\overline{\mu}}\overline{\mu} + e^{\overline{t}/\overline{\mu}}\,\overline{\mu}^3 + e^{\overline{t}/\overline{\mu}}\overline{t} + e^{\overline{t}/\overline{\mu}}\,\overline{\mu}^2\overline{t} + \overline{\mu}\cos(\overline{t}) - \overline{\mu}^3\cos(\overline{t}) - 2\overline{\mu}^2\sin(\overline{t})\right)}{(1+\overline{\mu}^2)^2} \tag{12}$$

$$\overline{x}'(\overline{t}) = \frac{e^{-\overline{t}/\overline{\mu}}\,\overline{\mu}\,\overline{V}\left(2e^{\overline{t}/\overline{\mu}}\overline{\mu^2} + \frac{e^{\overline{t}/\overline{\mu}\overline{t}}}{\overline{\mu}} + e^{\overline{t}/\overline{\mu}}\overline{\mu}\overline{t} - 2\overline{\mu}^2\cos(\overline{t}) - \overline{\mu}\sin(\overline{t}) - \overline{\mu}^3\sin(\overline{t})\right)}{(1+\overline{\mu}^2)^2} - \frac{e^{-\overline{t}/\overline{\mu}}\,\overline{V}\left(-e^{\overline{t}/\overline{\mu}}\overline{\mu} + e^{\overline{t}/\overline{\mu}}\,\overline{\mu}^3 + e^{\overline{t}/\overline{\mu}}\overline{t} + e^{\overline{t}/\overline{\mu}}\,\overline{\mu}^2\overline{t} + \overline{\mu}\cos(\overline{t}) - \overline{\mu}^3\cos(\overline{t}) - 2\overline{\mu}^2\sin(\overline{t})\right)}{(1+\overline{\mu}^2)^2} \tag{13}$$

The initial vacuum result is then recovered when $\mu \to \infty$, giving

$$\lim_{\overline{\mu}\to\infty} \overline{x}(\overline{t}) = \overline{V} - \overline{V}\cos(\overline{t}) \tag{14}$$

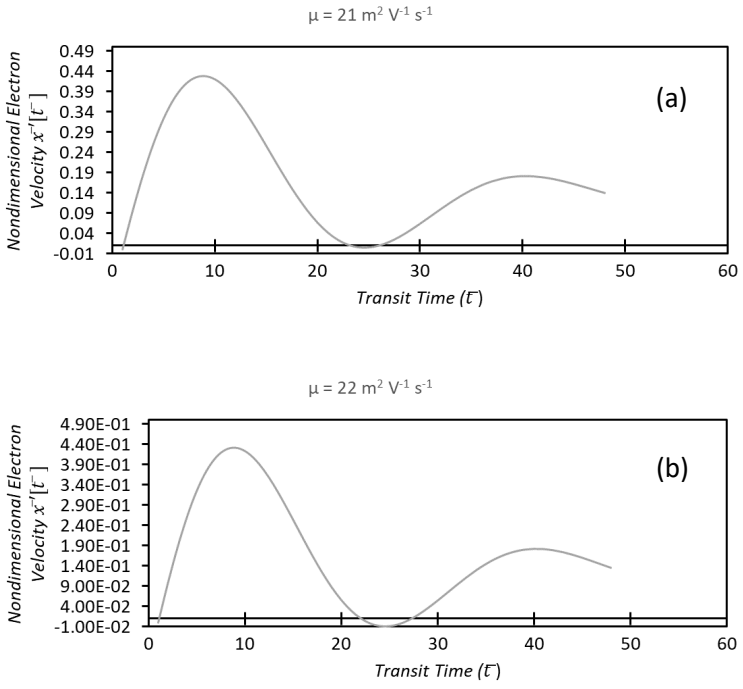

Figure 2. (a) Nondimensional electron velocity as a function of transit time ($\overline{t}$) at $\mu = 21\ \mathrm{m^2V^{-1}s^{-1}}$. (b) Nondimensional electron velocity as a function of transit time at $\mu = 22\ \mathrm{m^2V^{-1}s^{-1}}$.

Using the derived results, as seen in equations (12) and (13), we assessed how changing $\bar{\mu}$ changes the traditional Hull cutoff condition. Figure 2 compares different electron mobility values and how they impact electron trajectory. On the left, an electron mobility value of $21\ \mathrm{m^2V^{-1}s^{-1}}$ eliminates "traditional" magnetic insulation and the electron do reach the anode at zero velocity during their first pass. On the right, and electron mobility value of $22\ \mathrm{m^2V^{-1}s^{-1}}$ attains the "traditional" Hull cutoff condition of reaching the anode with $x'(\tau) = 0$. Inspection of these plots shows that there must be an extreme case for which magnetic insulation is maintained. To derive this extreme case, the nondimensional electron velocity equation (13) is simplified and rewritten as

$$\bar{x}'[\bar{t}] = \frac{e^{-\bar{t}/\bar{\mu}}\,\bar{\mu}\,\bar{V}\left\{e^{\bar{t}/\bar{\mu}} + \sqrt{\bar{\mu}^2 + 1^2}\,\sin\left[\bar{t} + \arctan\left(-\bar{\mu}^{-1}\right)\right]\right\}}{(1 + \bar{\mu}^2)} \tag{15}$$

This equation actually contains within itself two conditions for achieving the extreme case of reaching and anode with $x'(\tau) = 0$ on its first pass. The first condition arises by matching the exponential component of the nondimensional electron velocity with the magnitude of the sinusoidal component to yield

$$e^{\bar{t}/\bar{\mu}} = \sqrt{\bar{\mu}^2 + 1^2}. \tag{16}$$

The second condition equates the phase of the sinusoidal term to its maximum negative value

$$\bar{t} + \arctan\left(-\bar{\mu}^{-1}\right) = \frac{3\pi}{2} \tag{17}$$

The third condition for the Hull cutoff is the standard transit time condition, given by

$$\bar{x}[\bar{\tau}] = 1 \tag{18}$$

Through this simplification of the nondimensional electron velocity, three equations are derived and are used to solve for the three unknowns of this extreme case for the Modified Hull cutoff condition: nondimensional electron mobility, transit time, and magnetic field as defined below.

$$\bar{\mu} = 3.70217, \bar{t} = 4.9762$$

$$B = 0.176146\,T$$

$$\mu = 21.0177\ \mathrm{m^2V^{-1}s^{-1}}$$

Where dimensional electron mobility was derived using the scaling parameters defined earlier.

Simulation analysis and results. Along with theory derivation, simulations were also utilized to examine anode-cathode gap conditions. Specifically, simulations were conducted using constant electron mobility and varying magnetic field values along with those conducted using constant magnetic field and varying electron mobility values. Using the one-dimensional (1-D), three-dimensional velocity (3-v) particle-in-cell simulation code (XPDP1) [17] with the incorporation of electron mobility, we determined the electron transit time and electron trajectories. Analysis demonstrated that electron mobility and magnetic field have a strong influence on transit time, especially at magnetic fields above the Hull Cutoff and low mobility values. These findings are consistent with XPDP1 simulations displaying increased transit times with increasing pressure (which corresponds to decreasing electron mobility) [2].

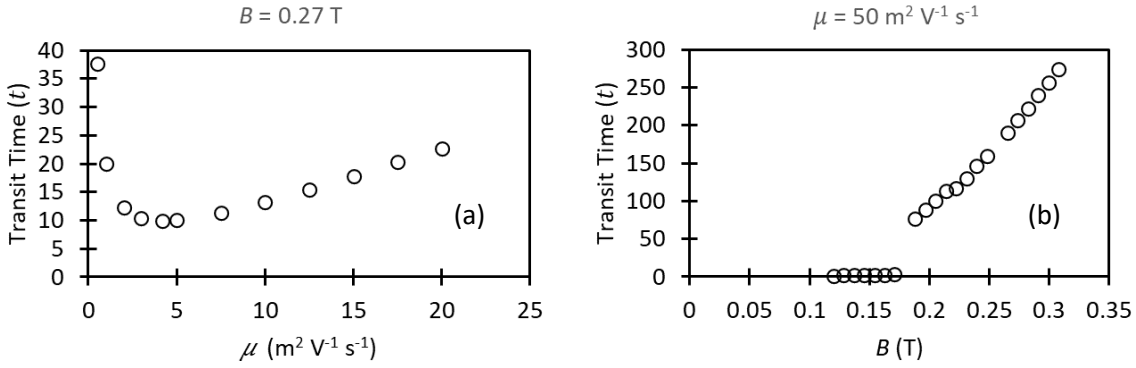

Figure 3. (a) Dimensionless transit time $\bar{t}$ as a function of electron mobility μ with constant magnetic field B. (b) Dimensionless transit time ($\bar{t}$) as a function of magnetic field B with constant electron mobility μ.

Figure 3 displays plots at constant magnetic field and constant electron mobility to display the influence on transit time along with the "jump" that occurs at low electron mobility and high

magnetic field. This large increase in transit time is due to looping electron trajectories that occur at high magnetic fields above the Hull cutoff, which prolong the electron excursion. These plots also suggest a possible "bifurcation" or "transition" point located at the Modified Hull cutoff due to the onset of electron loops. Additionally, the electron trajectories and transit times obtained using XPDP1 simulations and theory agreed well, as shown in Fig. 4.

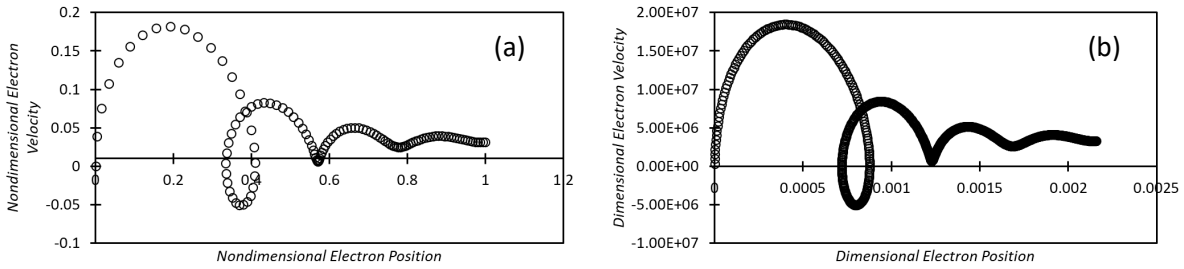

Figure 4. (a) Theoretically calculated and (b) simulated nondimensional electron velocity as a function of nondimensional electron position.

Conclusion

In summary, we demonstrated that introducing a finite electron mobility caused an electron emitted from the cathode to reach the anode; however, the traditional Hull cutoff condition still plays a significant role in characterizing the transit time of the electron. We derived a condition for electron mobility below which the electrons must loop before satisfying the traditional Hull cutoff condition, leading to a significant increase in transit time for magnetic fields above the threshold. This behavior is consistent with previous XPDP1 simulations demonstrating increasing transit times with increasing pressure (corresponding to decreasing electron mobility) [2]. Future studies include performing a parametric study of the modified Hull cutoff condition using theory and varying gap distances, voltages, and magnetic fields. Fluid models, such as SOMAFOAM [18], may further elucidate behavior at higher pressures or larger gaps in a more computationally efficient manner than particle-in-cell simulations.

Acknowledgments

This material is based upon work supported by the Sandia National Laboratories (SNL) and a Purdue Doctoral Fellowship. Sandia National Laboratories is a multimission laboratory managed and operated by National Technology & Engineering Solutions of Sandia, LLC, a wholly owned subsidiary of Honeywell International Inc., for the U.S. Department of Energy's National Nuclear Security Administration under contract DE-NA0003525. This paper describes objective technical results and analysis. Any subjective views or opinions that might be expressed in the paper do not necessarily represent the views of the U.S. Department of Energy or the United States Government.

Competing Interests:

The authors declare no competing interests.

[1] PJ Christenson and YY Lau, "Transition to turbulence in a crossed-field gap", Phys. Plasmas **1**, 3725-3727 (1994).

[2] B. S. Stutzman and J. W. Luginsland, "Loss of magnetic insulation in a crossed-field diode: Ion and collisional effects," IEEE Trans. Plasma Sci. **38**, 2010–2015 (2010).

[3] A. W. Hull, "The effect of a uniform magnetic field on the motion of electrons between coaxial cylinders," Phys. Rev. **18**, 31–57 (1921).

[4] P. J. Christenson, "Equilibrium, stability, and turbulence in cycloidal electron flows in crossed electric and magnetic fields," Ph.D. dissertation (University of Michigan, 1996).

[5] A. L. Garner, Y. Y. Lau, and D. Chernin, "Collapse of cycloidal electron flows induced by misalignments in a magnetically insulated diode," Phys. Plasmas **5**, 2447–2453 (1998).

[6] A. M. Darr, A. L. Garner, "Modifications of limiting current and magnetic insulation in a crossed-field diode by a series resistor," IEEE Access **10**, 60438-60446 (2022).

[7] Y. Y. Lau, J. W. Luginsland, K. L. Cartwright, and M. D. Haworth, "Role of ions in a crossed-field diode," Phys. Rev. Lett. **98**, 015002 (2007).

[8] M. S. Benilov, "The Child–Langmuir law and analytical theory of collisionless to collision-dominated sheaths," Plasma Sources Sci. Technol. **18**, 014005 (2009)

[9] A. M. Darr and A. L. Garner, “A coordinate system invariant formulation for space-charge limited current in vacuum,” Appl. Phys. Lett. **115**, 054101 (2019).

[10] S. D. Dynako, A. M. Darr, and A. L. Garner, “Incorporating resistance into the transition from field emission to space charge limited emission with collisions,” IEEE J. Electron Devices Soc. **7**, 650 (2019).

[11] A. M. Darr, C. R. Darr, and A. L. Garner, “Theoretical assessment of transitions across thermionic, field, and space-charge limited emission,” Phys. Rev. Res. **2**, 033137 (2020).

[12] S. A. Lang, A. M. Darr, and A. L. Garner, “Incorporating photoemission into the theoretical unification of electron emission and space-charge limited current,” J. Vac. Sci. Technol. B **39**, 062808 (2021).

[13] A. M. Loveless, A. M. Darr and A. L. Garner, "Theoretical linkage of thermionic field and space-charge limited emission for a vacuum crossed-field gap," IEEE Trans. Plasma Sci., Apr. 2022, in press.

[14] Y. Y. Lau, P. J. Christenson, and D. Chernin, “Limiting current in a crossed-field gap,” Phys. Fluids B **5**, 4486–4489 (1993).

[15] P. J. Christenson and Y. Y. Lau, “Transition to turbulence in a crossed-field gap,” Phys. Plasmas **1**, 3725–3727 (1994).

[16] P. J. Christenson and Y. Y. Lau, “One-dimensional modulational instability in a crossed-field gap,” Phys. Rev. Lett. **76**, 3324–3327 (1996).

[17] J. P. Verboncoeur, M.V. Alves, V. Vahedi, and C. K. Birdsall, “Simultaneous potential and circuit solution for 1D bounded plasma particle simulation codes,” J. Comput. Phys. **104**, 321-328 (1993).

[18] A. K. Verma and A. Venkattraman, “SOMAFOAM: An OpenFOAM based solver for continuum simulations of low-temperature plasmas,” Comp. Phys. Commun. **263**, 107855 (2021).